Agar/NaCl tissue phantom mimicking electrical properties of human body in low frequency spectrum

BSc Thesis

Bonne Bogaert, Luuk Mijjer & Mirthe Otter

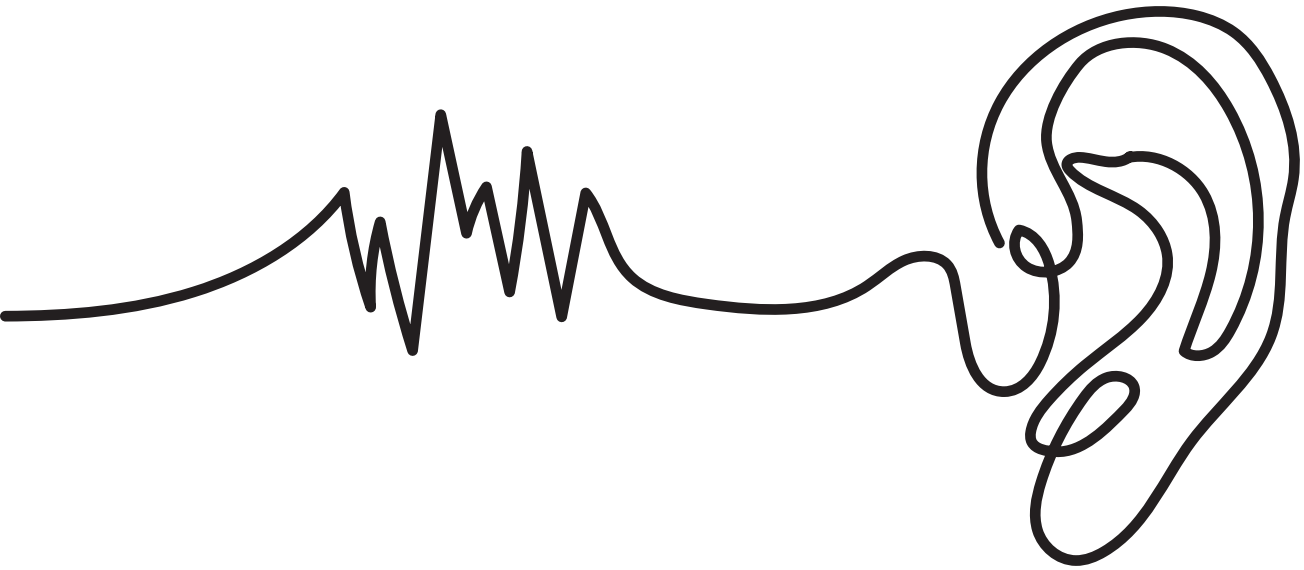

TU Delft

TU Delft

Agar/NaCl Tissue Phantom Mimicking Electrical Properties of Human Body in Low Frequency Spectrum

A Brain-Computer Interface Inside Your Earphones

by

Bonne Bogaert, Luuk Mijjer and Mirthe Otter

Bachelor Graduation Thesis

Student Number:	B. Bogaert	5107105
	L. Mijjer	4727207
	M. Otter	4771184
Project Duration:	April 19, 2022 - June 24, 2022	
Supervisor:	dr. T. Costa	TU Delft
	dr. D. Muratore	TU Delft
Daily Supervisor:	BSc. P. Burgar	TU Delft

Delft University of Technology

Faculty of Electrical Engineering, Mathematics and Computer Science

Electrical Engineering Programme

Abstract

This report details the design and development of an agar/NaCl gel-like tissue phantom mimicking the electrical properties of wet human skin. The skin phantom provides a reliable, reproducible testing ground for dry-contact polydimethylsiloxane (CNT/PDMS) electrodes, with the aim of recording electroencephalograms (EEGs) and stimulating brain activity in a controlled environment. These electrodes are being designed for the development of an in-ear brain-computer interface (BCI).
The electrical properties of biological tissue are referred to as the conductivity σ and permittivity ε and denote the ability for a material to conduct and trap electric charge respectively. These properties are frequency dependent and particularly for EEGs, a frequency range of 1-1000 Hz is of interest (with some added leeway). Wet skin hereby has a conductivity of around 0.1 Siemens to 0.2 Siemens in the 1-1000 Hz frequency range whereas the permittivity ranges from $5.7 \cdot 10^5$ to $5.2 \cdot 10^5$. Different agar and agar/NaCl solutions are created to try and obtain solutions with the mentioned electric properties. Specifically, NaCl is added to improve the conductivity and obtain a non-linear frequency response similar to that of human skin. The electrical properties of the phantoms were verified/measured using the parallel plate method. This method is essentially sandwiching a material under test (MUT) (in this case the fabricated gel-like agar and agar/NaCl solutions) between two conducting plates. This method is most suited for measurements in the lower frequency spectrum.
The skin phantom consisting of 3.04 mass fraction weight (wt.%) agar and 0.539 wt.% NaCl shows the closest similarity to the conductivity of wet skin. Namely, a conductivity of $\pm$ 0.1 Siemens to 0.45 Siemens in the frequency range of 1-1000 Hz. A decrease of 0.250 wt.% NaCl will most likely achieve the desired conductivity response of 0.1 Siemens to 0.2 Siemens in the frequency range of 1-1000 Hz. The skin phantom consisting of 3.00 wt.% agar and 1.02 wt.% NaCl showed the permittivity closest to that of wet skin, but might have been a noisy outlier. Its permittivity ranges from $10 \cdot 10^6$ and $7.5 \cdot 10^6$. This is still a large error margin from the desired $5.7 \cdot 10^5$ to $5.2 \cdot 10^5$. Additional fillers like glycine or Al powder need to be added to the solutions to obtain a permittivity close to that of wet human skin. Multi-day and difference in applied pressure measurements are performed to check the sensitivity and reproducibility of the phantoms. Applied pressure hereby has little to no influence whereas a longer life-span of the fabricated phantom shows a drastic decrease of the electrical properties of the phantoms after day 1. The changes then seem to settle. Worth mentioning is that the change is only drastic when the solution has a high conductivity. This is generally not the case for solutions with conductivities close to wet skin.

Preface

For the past two months we have devoted ourselves to the BSc graduation project of creating a tissue phantom. Being in the final phase of our Bachelor studies, this is the very last project that we have to complete successfully in order to earn a bachelor's degree in Electrical Engineering. We hope we delivered satisfactory.

These past two months have been experienced as instructive and challenging, in a good way. In addition to being able to apply theory and application-oriented disciplines included in the BSc curriculum, thanks to this project, we were able to seize the opportunity to gain knowledge of, to us, new but interesting application areas within the field of electrical engineering. We got acquainted with the complex structures and electrical properties of biological tissues, were introduced to the fabrication of tissue phantoms, and learned how to perform impedance measurements. This proves once again how widely applicable electrical engineering is.

We would like to express our gratitude to our main supervisor Tiago Costa, and daily supervisor Patricija Burgar, who guided us through this project, supported us in finding a lab spot, and were available to answer all of our questions. Furthermore, we would like to thank our supervisor Dante Muratore for proposing this project, and supervising the project group of which we were part as a subgroup. Finally we would like to thank Gandhi Wardhana, Niels Burghoorn, Filip Simjanoski, and all of our colleagues: Sam Aanhane, Chris Bot, Kees Broek, Arthur de Groot, Simon Molenkamp, Aurore de Spirlet, Jorn Teurlings, Joos Vrijdag and Bart Zuidema.

Bonne Bogaert, Luuk Mijjer & Mirthe Otter
Delft, June 2022

Contents

1

Introduction

Living cells and tissues of human beings and animals generate electric signals, also often referred to as bioelectrical signals. These signals reflect the physiological state of organs and/or tissues. Thus, detecting bioelectrical signals can be useful in the diagnosis of neurological diseases (epilepsy, tumours, and brain death among others). More so, stimulating bioelectrical signals in some way might be beneficial in treating said diseases. Methods have already been developed to detect bioelectrical signals. An example of this is electroencephalography (EEG). I.e., the recording of the brain's bioelectrical signals. Typical scalp-EEG systems have their limitations, however, as they are bulky, tethered (see Figure 1.1) and require electrodes to be attached to the scalp via the use of a conductive gel.

Figure 1.1: Example of standard-issue equipment used to record EEGs with

This creates difficulty when trying to monitor brain activity over a long period of time. An example scenario is: when trying to monitor the on-set detection of epileptic events in a person when in a non-clinical environment (in their day-to-day life). Additionally, the conductive gel dries out over time and the electrode-skin contact can cause scarring. Recent developments, therefore, show an interest in brain-computer interfaces (BCIs): small wearable external devices that provide a direct communication link to the nervous system. In other words, wearable devices that can be used, for example, to monitor brain activity 24/7 in a non-clinical environment, prosthetic control, and/or even be used for consumer-related applications such as three-factor authentication. However, to create a desirable BCI for both patients and consumers, the BCI has to maintain a good appearance and has to avoid publicising illnesses. Thus, the scalp electrodes used in conventional EEG systems are not suited for this application. For this matter, the ability to record EEGs using dry-contact electrodes placed in and around the ear has been investigated in recent years. Specifically in and around the ear, because hair causes too much interference in EEGs when a conductive gel is not applied. Currently, the development of dry electrodes is still being min-maxed, and newly developed electrodes require extensive testing to determine their bio- and skin compatibility (and therefore their functionality in recording EEGs). It is unwise to perform these tests on in vivo subjects as the electrode-skin contact might cause irreversible damage to the skin.

Furthermore, in vitro human tissue is not readily available. For this reason, phantoms are often used. Phantoms are objects that mimic or imitate the electrical, mechanical, and/or physical properties of the human body, like tissue.

This BSc thesis is part of a bigger project that has the goal of creating a closed-loop system in an ear-EEG BCI. The system is supposed to authenticate the user of the BCI, detect epileptic seizures, and provide nerve stimulation to prevent or mitigate seizures. Figure 1.2 provides a visualisation of the system's sub-components; amongst which a phantom. This BSc thesis will look into the design of a sub-component: a phantom, such that carbon nanotube/polydimethylsiloxane (CNT/PDMS) composite-based dry electrodes (to be placed inside the ear BCI) can be tested. Particularly, such that the electrodes can be tested for their functionality in recording EEGs and stimulating brain activity.

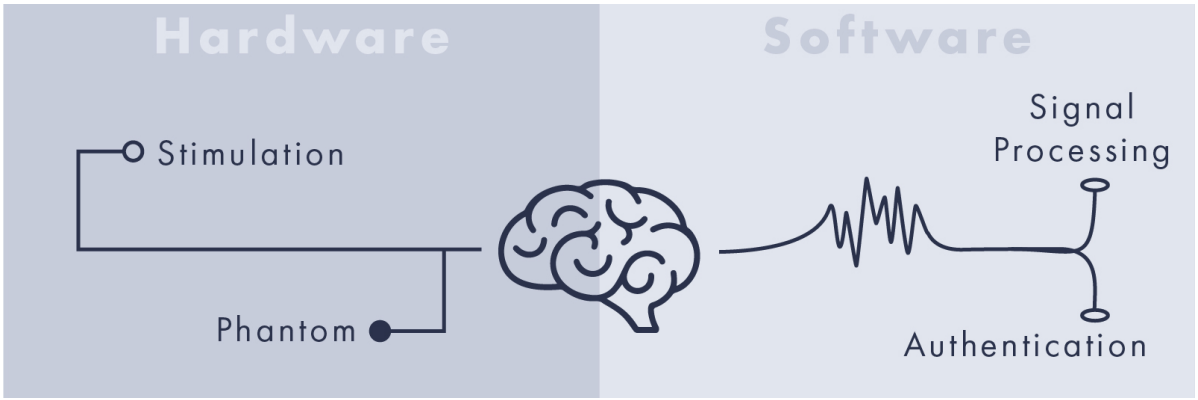

Figure 1.2: Overview of sub-components to be used in a closed-loop system for an ear-EEG BCI design

Firstly, chapter 2 provides some background information on the electrical properties of biological tissue. Chapter 3 will hereby give an analysis of the electrical properties of human tissue and what has currently been achieved by others when it comes to mimicking human tissue. The chapter concludes with a problem definition that is realistically achievable in this BSc Thesis. Sub-sequentially chapter 4 provides the requirements needed to solve the problem. Chapter 5 describes the first process steps in solving the problem: the design of the phantom(s). Chapter 6 explains the measurement technique used to extract the phantom's electrical properties to verify the correctness of the fabricated phantom(s). Chapter 7 discusses the results obtained from the measurements and finally, chapter 8 provides a conclusion and recommendations for future work.

2

Background knowledge

The electrical properties of any material can be separated into two categories: conducting and insulating. In a conductor, electric charges move freely in response to an applied electric field (electric force). The opposite occurs in insulators: electric charges are fixed and not free to move. Most materials, including biological tissue, show both conductive and insulating behaviours [25]. In other words, biological tissue shows an ability to trap electric charge and shows an ability to move electric charge. This is denoted by the permittivity ε and conductivity σ, respectively. A simple circuit model of tissue is hereby often considered as a capacitor in parallel with a conductor (see Figure 2.1) and referred to as the Debye-type [25].

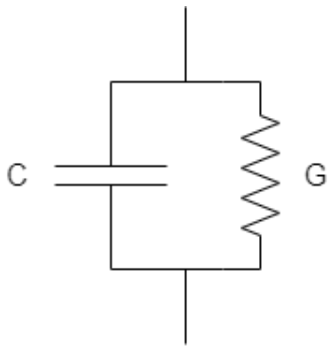

Figure 2.1: Equivalent circuit of biological tissue using the Debye-type

Given tissue with a cross-sectional area A, and thickness d, the relation of absolute permittivity ε to the capacitance C of a capacitor is described by Equation 2.1 whereas the conductivity σ is related via the conductance G of the conductor described by Equation 2.2.

$$C = \varepsilon \frac{A}{d} \tag{2.1}$$

$$G = \sigma \frac{A}{d} \tag{2.2}$$

It is worth mentioning that the absolute permittivity ε is the product of the relative permittivity of the material ε_r and the permittivity of vacuum ε_0 (constant $8.854 \cdot 10^{-12}$ F/m). This is also described by Equation 2.3.

$$\varepsilon = \varepsilon_r \varepsilon_0 \tag{2.3}$$

Furthermore, when applying an AC voltage, a frequency-dependent permittivity $\hat{\varepsilon}$ and conductivity $\hat{\sigma}$ can be defined as Equation 2.4 and Equation 2.5 [25].

$$\hat{\varepsilon} = \varepsilon_r - \frac{\mathrm{i}\sigma}{\omega\varepsilon_0} = \varepsilon_r' - \mathrm{i}\varepsilon_r'' \tag{2.4}$$

$$\hat{\sigma} = \sigma + \mathrm{i}\omega\varepsilon \tag{2.5}$$

with $\varepsilon_r' = \varepsilon_r$ and $\varepsilon_r'' = \sigma/(\omega\varepsilon_0)$. Here, ε_r is the relative permittivity, ε_0 the permittivity of vacuum, $i = \sqrt{(-1)}$ and σ the DC conductivity.

Another model used to describe biological tissue is the Cole-Cole model which is considered more accurate compared to the Debye-type [25]. For the Cole-Cole model, the capacitor in the Debye-type is replaced by a Constant Phase Element (CPE) with a complex-valued impedance (see Figure 2.2).

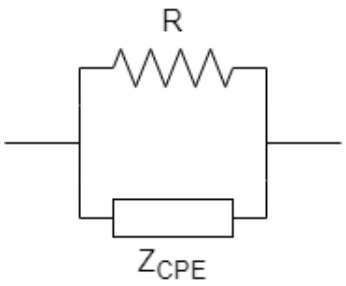

Figure 2.2: Equivalent circuit of biological tissue using the Cole-Cole model

3

State-of-the-art analysis

The fabrication of tissue phantoms has been widely researched and is typically categorised into 3 types when considering the head. These are the homogeneous phantoms (single layer), multi-layer phantoms representing the scalp, skull and brain, and real-tissue phantoms (donor tissue from humans and/or animals) [2, 3, 5, 7, 13–17].
Phantoms that require donor tissue are not considered applicable for this BSc Thesis but are still a noteworthy mention. A 3D skin model can be cell-cultured via the use of bioreactors [1]. Bioreactors provide biochemical and physical regulatory signals to cells and encourage them to undergo differentiation. Simply said, stimulates cells for growth and regeneration such that in vitro tissue can be formed. The main use when engineering tissue via bioreactors is to perform grafts, but the engineered tissue can also be used as external organ support devices or provide reliable model systems [4]. Thus, in the application of phantoms, skin can be modelled via the use of bioreactors as long as donor tissue/cells are available to do so.
When considering the other two phantom types, the single-layer- and the multi-layer-phantoms, gel-based solutions are mainly used. Gel-based phantoms are favourable as they are high in water content (just like the human body) and provide selective "tuning" of the electrical properties by changing said water content [13, 14]. In other words, the conductive and dielectric properties of gel phantoms can be adjusted by adding fillers. Hereby, a wide variety of materials has been documented to fabricate tissue phantoms. Some materials used are wax, silicon, plastic clay, plastic moulds and gelatin; with gelatin being the most common one by far [13]. Fabricating tissue phantoms via the use of gelatin seems logical, as gelatin is obtained from various animal by-products. However, the use of gelatin can be considered animal testing/non-animal friendly and is therefore sometimes avoided. A popular alternative to gelatin is Agaragar (agar in short). Agar is a jelly-like substance made from algae, and just like gelatin, agar has similar electrical properties to that of human tissue [17].

3.1. Phantom design

Sodium chloride (NaCl), also known as salt, is essential to the human body and is used to regulate the electrolyte balance of fluids in a person's body. Thus, to construct gel-based phantoms that mimic human tissue, NaCl is often added to the gel. There has been shown that varying concentrations of NaCl relative to gelatin or agar powder shift the solution's phase/frequency response profile [17]. Gelatin/NaCl solutions show similar non-linear frequency dependency to that of human tissue. Agar/-NaCl solutions also show similar properties. However, a lesser similarity when compared with the gelatin/NaCl-based solutions. In [15] it is mentioned that the same concentration of NaCl in gelatin-based phantoms showed higher dielectric properties than that in agar-based phantoms at all frequencies.

According to Thomas J. Yorkey [22], the relationship between NaCl concentration and the agar's conductivity σ is given by:

$$\left(\sigma, {}^{S}/\mathrm{m}\right) = 200\,(S \cdot mL/m \cdot g) \times \frac{\text{grams of NaCl)}}{(\text{ solution volume }, mL)} \tag{3.1}$$

According to D. Bennett [17] that relationship can be expressed as the frequency-independent linear model given below.

$$\left(\sigma, {}^{S}/\mathrm{m}\right) = 215 \times \frac{(\text{ grams of NaCl})}{(\text{ solution volume, mL})} + 0.0529 \tag{3.2}$$

With these expressions, agar/NaCl solutions can be modelled to have desired conductivities. The range of conductivities for human tissue is further mentioned in section 3.3. For now, some examples of previously fabricated gelatin- and agar-NaCl tissue phantoms are given below.

- Muscle tissue has been mimicked by mixing gelatin powder and agar powder with deionized water [15]. Aqueous NaCl was then added to improve conductivity such that the solution had similar conductive properties as muscle tissue. Glycine and aluminium (Al) powders were fillers added to increase the permittivity such that the solution had similar dielectric properties when compared to muscle tissue.
- Three phantom heads were fabricated using agar [16]. A one-layered spherical phantom, a three-layered spherical phantom and a human MRI-based three-layered phantom. The one-layered phantom represented the brain, whereas the three-layered phantoms represented the scalp, skull and brain of a human. Plastic moulds were fabricated to recreate a three-layer shell structure. These moulds were built using a 3D printer. The moulds were then filled with three different Agar/NaCl mixtures containing isotropic permittivities close to the scalp, skull and brain.

3.2. Frequency range

The electrical properties of tissues are frequency-dependent as mentioned in chapter 2. In the application of ear-EEG BCIs, it is therefore important to know the frequency range of interest. EEGs consist of waveforms and they can be characterised by factors such as amplitude, occurring location, continuity of waveform rhythm and frequency. Hereby, according to [23], EEG waveforms are most frequently characterised by their frequency spectrum. Four main frequency waveforms are observed in EEGs: delta, theta, alpha and beta waves. Delta waves range from 0-4 Hz and are mostly present when a person is in deep sleep or are caused by abnormalities such as tumours. Theta waves range from 4-7 Hz and are more prominent in childhood than adulthood. They are also present when someone experiences drowsiness. Alpha waves range from 8-12 Hz and are the hallmark frequency of normal awake adult brains. Beta waves range from 13-30 Hz and are associated with muscle contractions (movement). Some other waveforms like sigma (12-16 Hz) and gamma (>30 Hz) are present, but are not as commonly observed as the delta, theta, alpha and beta waveforms. an EEG frequency spectrum can thus be considered to be around 1-1000 Hz (with some added leeway).

3.3. Electrical properties of human tissue and electrode-skin interface

In EEGs, bioelectrical signals travel through the scalp, skull and brain. However, for dry electrodes, electrode-skin contact is critical in observing noise-free EEGs [5]. The electrode-skin contact is hereby mostly influenced by the electrical and mechanical properties of the skin. Additionally, the skin is one of the most resistive tissues in the human body [25]. Therefore, to provide a satisfactory testing ground for dry-contact electrodes, it is best to have the phantom mimic skin. This section will therefore describe the electrical properties of skin rather than also including the skull and brain.

Skin tissue can be subdivided into different layers. In short, these different layers are the epidermis (pigment cells), the dermis (nerve endings, sweat glands and hair follicles) and subcutaneous tissue (fat, blood vessels and nerves). The outermost layer of the epidermis is the stratum corneum. The stratum corneum is the uppermost layer of the skin and acts as a barrier to keep out contaminants. It consists of hydrophobic (water-fearing) lipids and is the reason why skin is one of the most resistive tissues in the human body. However, when wet, sweaty or bypassed, the conductance of the stratum corneum increases considerably [32]. It is speculated that the reason for this is that the electric charge in the skin only moves through the sweat glands [33]. Furthermore, water gathering on the surface of the skin also improves the interface between skin and electrodes as the conductivity of water is higher than that

of air providing a better interface medium between skin and electrodes. The electrical properties of skin are thus often subdivided into the categories of wet skin and dry skin. Some other factors that influence the resistivity of the skin are electrodermal response [34], the temperature [25], and in the application of ear BCIs, cerumen inside an ear. P. Akshay et al. [34] measured an 86% decrease in measured resistivity after removing normal levels of cerumen in the application of dry-contact electrode use. The factor applied pressure is also of importance when considering the electrode-skin interface [6]. Applying light to moderate pressure results in good electrode-skin contact. Applying too much force will result in an increase in resistivity.

S Gabriel, R. W. Lau and C. Gabriel [10] provided a prediction model for the electrical properties of human tissues given literature data that was present at the time and based on the Cole-Cole model described in chapter 2. Literature data will be considered here, as the prediction model is not reliable for the lower frequency ranges due to the scarce data present (also mentioned in [10]).

- The reported literature data for dry skin conductivity ranges from $1 \cdot 10^{-5}$ Siemens to $5 \cdot 10^{-5}$ Siemens in the frequency range of 1-1000 Hz
- The reported literature data for dry skin relative permittivity ranges from 3700 to 3100 in the frequency range of 1-1000 Hz.
- The reported literature data for wet skin conductivity ranges from 0.11 Siemens to 0.2 Siemens in the frequency range of 1-1000 Hz
- The reported literature data for wet skin relative permittivity ranges from $5.7 \cdot 10^5$ to $5.2 \cdot 10^5$ in the frequency range of 1-1000 Hz.

3.4. The problem definition

The problem at hand is to model the electrical characteristics of human skin. As mentioned in section 3.3, wet skin improves the conductivity of the skin and the electrode-skin contact interface; therefore lessening the noise observed in EEG recordings. The opposite, modelling for dry skin, provides a ground for worst-case scenario testing, but requires very precise equipment to do so. In section 3.3 was mentioned that dry skin conductivity ranges from $1 \cdot 10^{-5}$ Siemens to $5 \cdot 10^{-5}$ Siemens in the lower frequency spectrum. This is very difficult to obtain. This BSc thesis will therefore look into a phantom representing wet skin. The wet skin model to be considered here is time-invariant rather than time-variant. A time-invariant system provides a controlled environment and reproducible results. This is significantly more difficult to achieve with a variant system and unrealistic for this BSc Thesis. The skin is also to be modelled as either single-layered or multi-layered. This will be further discussed in chapter 5. The skin model needs to simulate for applications related to the EEG spectrum. This requires mimicking the electrical properties in the lower range of the frequency spectrum ($\pm$1-1000 Hz). Finally, all these factors need to be applicable to stimulate testing for ear BCI applications. Therefore, the phantom can be shaped in the form of an average-sized human ear.
The global design process is visualised in Figure 3.1. All action points have been identified herein in sequence, and will subsequently be discussed in a fluent way in the coming chapters of this BSc Thesis. Starting with the objectives in chapter 4, which will be precisely defined in the Programme of Requirements.

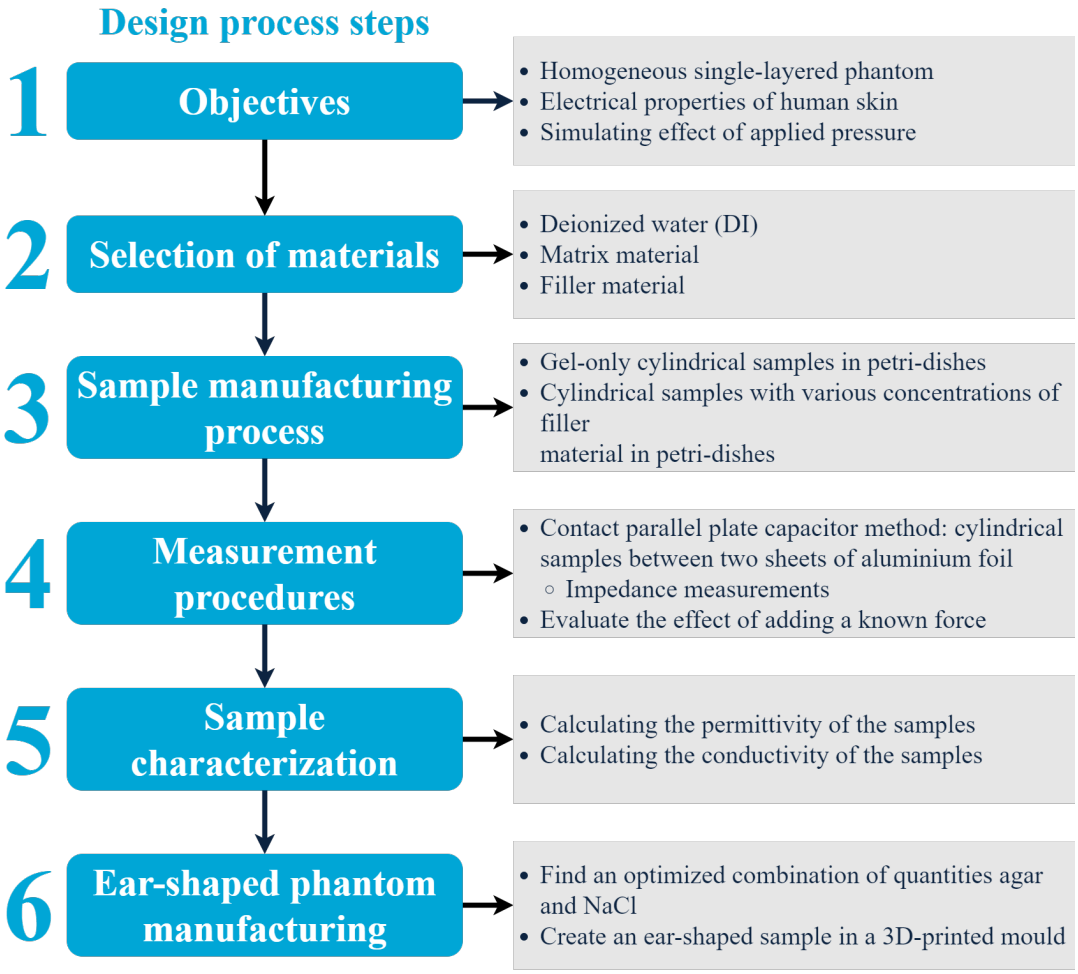

Figure 3.1: Flowchart of the design process steps

4

Programme of requirements

The goals of the BSc Thesis are established and framed in the Programme of Requirements. In the coming sections, the objectives will be described in the form of functional and non-functional requirements (the definition of which will be explained in more detail). These objectives for the end product are based on the problem definition described in section 3.4.
This chapter thus deals with the first of the six steps of the design process of Figure 3.1. The five subsequent steps describe how the final product is formed and will be handled in the upcoming chapters.

4.1. Functional requirements

Functional requirements, given in Table 4.1, are requirements that are fundamental for an acceptable end result.

Table 4.1: Functional requirements: mandatory requirements are classified as A and trade-off as B.

Number	Name	Description
A.1	function	The phantom must support testing the functionality of a dry electrode to be implemented in an ear-EEG BCI.
A.2	function	The phantom must support testing the effect of applied pressure by measuring the changes in conductivity when different known forces are applied to the phantoms.
A.3	performance	The phantom must have the same relative permittivity as wet human skin at a constant temperature and pressure with an accuracy of 90% in the spectrum extending from 1 Hz to 1 kHz ($5.7 \cdot 10^5$ to $5.2 \cdot 10^5$).
A.4	performance	The phantom must have the same conductivity as wet human skin at a constant temperature and pressure with an accuracy of 90% in the spectrum extending from 1 Hz to 1 kHz (0.1 to 0.2 Siemens).
A.7	dimension	The phantom must have the form and dimensions of an average human ear.
A.8	dimension	The phantom must have an ear canal of at least 1.5 cm deep to perform in-ear experiments.

4.2. Non-functional requirements

The non-functional requirements, given in Table 4.2, describe the attributes and qualities which the end-product must have or that increase the satisfaction of the end-user if the end-product complies with these requirements.

Table 4.2: Non-functional requirements: mandatory requirements are classified as C and trade-off as D.

Number	**Name**	**Description**
C.1	ethics	The phantom must be composed of animal friendly materials.
C.2	safety/law	The procedure should be performed in a safe environment following the lab rules/instructions.
D.1	lifetime	The phantom should keep its electrical properties for at least 7 days with a maximal decay of 5%.
D.2	price	The price of the phantom should preferably be kept to a minimum.
D.3	performance	All equipment used (3D-printer, impedance meter, weighing scale and calipers amongst others) should be as precise as possible.

5

Skin phantom design

The skin phantom to be designed can either be modelled multi-layered or single-layered (homogeneous). There are various reasons one can consider modelling for multi-layered phantoms, but the main reason would be to single out the effects caused by the different layers of the human skin. This is not of interest for EEG applications as the electrode attached to the skin observes the entire skin impedance at all times. Therefore, there is no need for distinguishing the different layers of the skin. However, one noteworthy possibility that can be considered in EEG recordings is the effect of the outermost layer of the epidermis: the stratum corneum. As previously mentioned in section 3.3, the stratum corneum is one of the reasons skin can be considered one of the most resistive biological tissues. There has been shown that for low frequencies (<10 kHz), the stratum corneum makes up for ±50% of the total skin impedance [26]. Therefore, for low frequencies, one could consider a two-layered phantom model containing the stratum corneum in series with the remainder skin layers. In the application of the BCI however, the result would mean regularly peeling off the stratum corneum layer to reduce the total impedance, which seems inconvenient for its users and thus does not support a long-term solution. Rather favourable is to model the skin phantom to be single-layered.

5.1. Selection of sample materials

For the fabrication of a tissue-mimicking material, agar powder is selected as a matrix material (a constituent of composite material) to achieve the desired gel-like substance. The plant-based material agar is a jelly-like substance made from algae and was chosen over gelatin for ethical reasons (animal-friendly). As mentioned in chapter 3, its electrical properties are similar to the human skin, and, because of its high water content, can be "tuned" by adding filler materials to the agar mixture [15]. Promising filler materials are NaCl, Al powder and glycine (Aminoacid), as they will add to the electrical conductivity as well as the relative permittivity of the phantom. In particular, adjusting the NaCl concentration is suitable for tuning the impedance [14], as well as ensuring a non-linear frequency response of the phantom [9].

5.2. Ear-shaped mould

Since the ear is the main part of interest, it is useful to get the phantom in the shape of the human ear to perform in-ear experiments with the electrodes. To achieve this, an ear-shaped mould is created to pour the agar into. Since the ear has a very organic shape, it is not possible to pull the result straight out, so the mould is divided into two pieces. Teflon spray can be used to pull the result out easier. The first iteration of the mould has been designed in the free CAD program Fusion 360 and a Creality Ender 3 printer is used with a minimal layer height of 0.12 mm. It has been taken into account that the design complies with requirement A.8 of section 4.1.
Figure 5.1 shows the result of the first printed iteration. An array of elastics around the two sub-moulds keeps the position the same during the moulding process and the boundary line width is reduced by sanding the parts and if necessary, silicone spray can be used to temporarily close the gap during the congealing process.

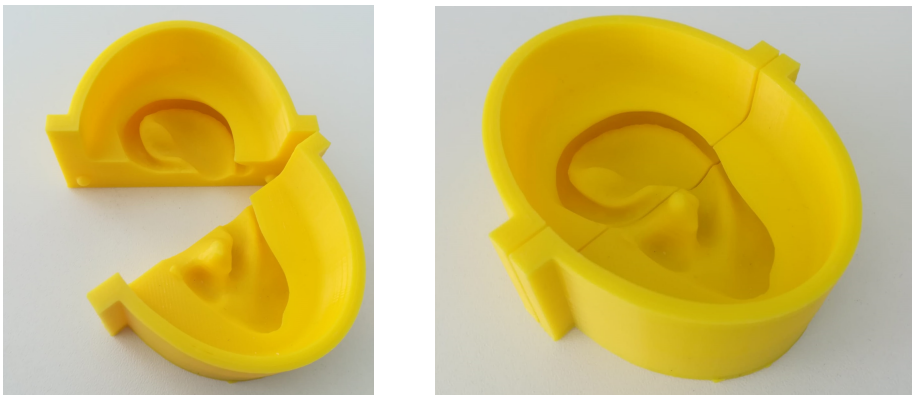

Figure 5.1: 3D-printed ear mould

5.3. Phantom fabrication

First, a batch of gel-only samples is created by mixing various concentrations of agar powder (E 406) with deionized water (DI) for the characterisation of the dielectric properties of agar. DI by itself is not conductive, because, as the name implies, the ions are removed from the water. The agar powder and DI were weighed by a mass fraction (wt%) with a Fisherbrand Analytical Series. The quantities of these gel-only samples are shown in rows 1 to 6 of Table 5.1. The range of concentrations of agar used matches [2, 15, 20]. Thin cylindrical samples were manufactured in Petri-dishes for electrical tests with an area of 113 cm^2. The solution was stirred with a magnetic stir bar (Spinbar magnetic stir bar, PTFE-coated, polygon, size 6 mm x 15 mm, white) on a stirring hotplate (Thermo Scientific Cimarec$^+$) for 1 minute at 400 RPM in a 250 ml beaker and then heated to 90 ℃ while stirring at 600 RPM. To research the effects of adding filler materials to the phantom sample, various quantities of NaCl (table salt) are added to the solutions (rows 7 to 16 in Table 5.1), while stirring at the lowest speed for three more minutes. The range of concentrations of NaCl used matches the literature [2, 3, 13, 14] and is based on Equation 3.1. However, this step can be skipped for gel-only solutions. Afterwards, the solutions are transferred to the mould or Petri-dishes covered with Teflon spray (Griffon PTFE spray) to prevent the samples from sticking to the dish/mould. After at least 3 hours of congealing at room temperature, the samples were removed. The thickness of the samples was measured with an analogue calliper with 0.1 mm precision, and is 8 mm. Finally, they were stored in the fridge at 2 ℃, to minimise water evaporation. This fabrication method is in line with methods used in other literature [15, 21] and is visualised in Figure 5.2.

Table 5.1: Table showing quantities used to produce samples, given in mass fraction weight (wt.%).

Solution #	Agar wt.%	NaCl wt.%
1	1.01	0
2	1.40	0
3	1.80	0
4	2.21	0
5	2.61	0
6	3.01	0
7	3.04	0.539
8	3.00	0.763
9	3.00	1.02
10	3.02	1.28
11	3.02	1.50
12	3.01	1.75
13	2.02	0.503
14	2.01	1.00
15	2.01	1.50
16	1.03	0.506

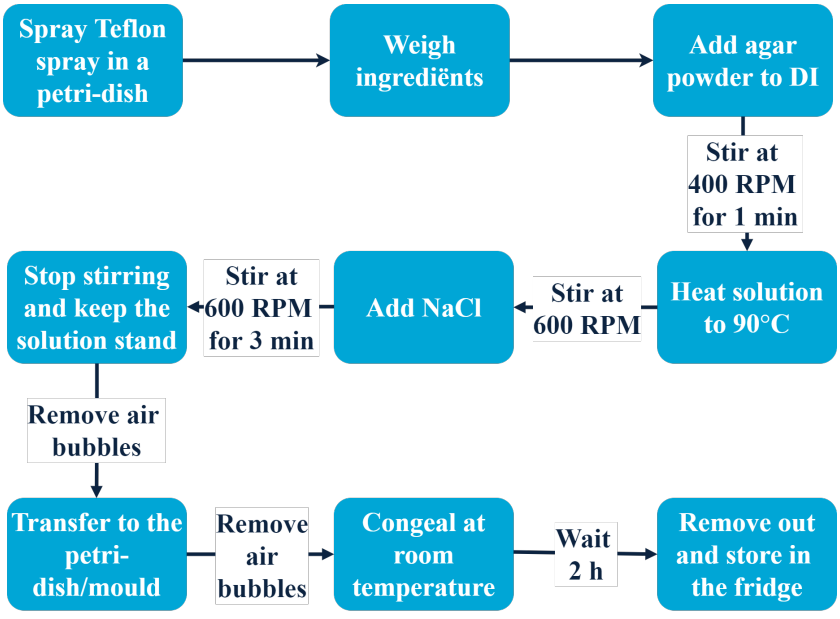

Figure 5.2: Flowchart phantom sample fabrication

6

Measurement technique

With the phantoms fabricated, measurements need to be performed to verify the correctness of the phantom's electrical properties. There are various measurement techniques used to extract the electrical properties. Some examples are the coaxial probe, transmission line, free space, resonant cavity and parallel plate methods [28]. The choice of technique hereby depends on factors like frequency of interest, material properties, material form (liquid and solid amongst others), sample size, contacting or not-contacting and temperature. For the phantom application, a large limiting factor is the frequency of interest. All of the above methods, besides the parallel plate method, are best used for frequencies around or larger than 50 MHz [28, 29]. As mentioned in section 3.4 and chapter 4, the frequency range of interest is that of EEG applications (with some added leeway) ranging from 1-1000 Hz. Because of that, the parallel plate method is most suited to measure the phantom's electrical properties. Other important factors to be considered for this method are the sample size and the form of the material (further discussed in section 6.3).

6.1. Contacting parallel plate method

A typical capacitor is formed of two conducting sheets with an insulator in between. The same principle holds for the contact parallel plate method. It consists of two conducting parallel plates with a material under test (MUT) sandwiched in between; thus forming a capacitor. In this case, the materials under test are the fabricated phantom solutions. When an AC voltage is applied to the plates, charge gathers on the surface of the plates and remains there; energy is stored. An ideal capacitor hereby has no losses. It only stores and releases energy. However, in practice, biological tissue is not a perfect insulator (also denoted as a dielectric) [25]. They in fact have some ability to conduct charge and some energy dissipation occurs. Biological tissues therefore show an ability to trap electric charge (permittivity ε) and show an ability to move electric charge (conductivity σ).

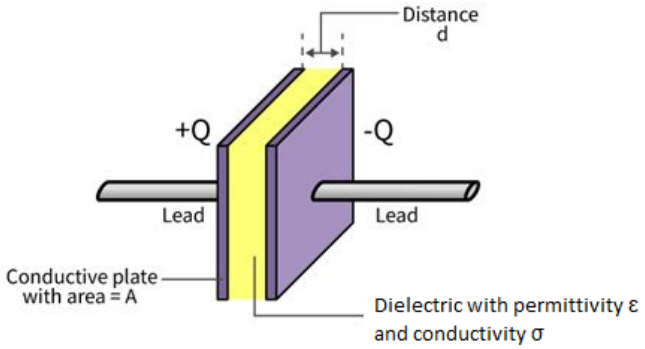

Figure 6.1: Parallel plate capacitor consisting of two conducting plates with area A and material under test (dielectric) sandwiched in between with thickness d.

When the MUT has an impedance Z > 100 KΩ, it can be considered equivalent to a capacitor with impedance $Z_c = \frac{1}{i\omega C}$ in parallel with a resistance R (see Figure 6.2) [31].

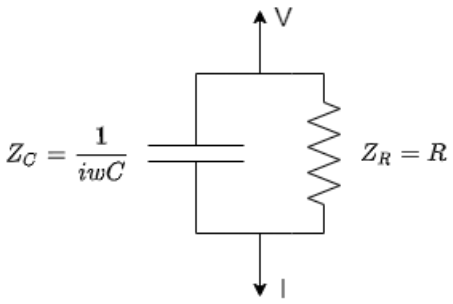

Figure 6.2: Equivalent parallel MUT circuit when its impedance Z > 100 KΩ

The impedance of this circuit is $Z = Z_c \parallel Z_R = \frac{R_p}{1+\omega^2 {R_p}^2 C_p^2} + i\frac{\omega R_p^2 C_p}{1+\omega^2 R_p^2 C_p^2}$ [31].

When the MUT has an impedance Z < 100 KΩ, it can be considered equivalent to a capacitor with impedance $Z_c = \frac{1}{i\omega C}$ in series with a resistance R (see Figure 6.3) [31].

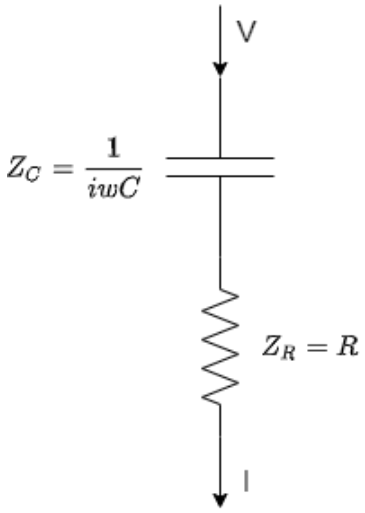

Figure 6.3: Equivalent serial MUT circuit when its impedance Z is < 100 KΩ

The impedance of this circuit is $Z = Z_c + Z_R = R + \frac{1}{i\omega C}$ [31].

6.2. Calculating the conductivity and relative permittivity

As previously mentioned in chapter 2, the standard formula for a capacitor is:

$$C = \varepsilon \frac{A}{d} \tag{6.1}$$

Where C is the measured capacitance in F, A is the contact area between a conducting plate and the MUT in m^2, d is the thickness of the MUT in m and ε is the absolute permittivity in F/m.

The absolute permittivity ε can also be defined as the product of the relative permittivity of the material ε_r and the permittivity of vacuum ε_0 (constant $8.854 \cdot 10^{-12}$ F/m) (see Equation 6.2).

$$\varepsilon = \varepsilon_r \varepsilon_0 \tag{6.2}$$

By substituting Equation 6.2 into Equation 6.1, the relative permittivity ε_r can be calculated as follows:

$$\varepsilon_r = \frac{Cd}{A\epsilon_0} \tag{6.3}$$

The conductivity σ is calculated via Equation 6.4 [25].

$$\sigma = \frac{d}{RA} \tag{6.4}$$

Where σ is the conductivity in S, A is the contact area between a conducting plate and the MUT in m^2, d is the thickness of the MUT in m and R is the measured resistance in Ω.

6.3. Parasitic effects

There are several parasitic effects that render a capacitor non-ideal. These effects need to be reduced as much as possible in order to consider the equations and the circuits above.

- **Fringing effect**: In practice, the electric field (or electric force) is formed when a voltage applied to a capacitor is larger than the actual contact area between conducting plates and the MUT. A non-uniform electric field also occurs at the edges of the capacitor. Therefore, the capacitance of the MUT is actually larger than described by the standard formula of a capacitor (Equation 6.1) causing some calculation errors. To be able to neglect fringing effects, the contact area of the samples and the conducting plates must be significantly larger than the thickness of the phantom sample (A » d). Furthermore, to further reduce fringing effects, a third conducting plate can be introduced. This is also mentioned as a guard. One of the two conducting plates is hereby reduced in size and the guard is placed on the edges next to this plate. A small insulating gap is to be present between the guard and the conducting plate to prevent the conduction of charge between the two. The flow of charge present due to the electric field at the edges will now be absorbed by the guards. The contact area between a conducting plate and sample is now the true area mentioned in Equation 6.1. Therefore, the standard formula for a capacitor (Equation 6.1 can be used more accurately.

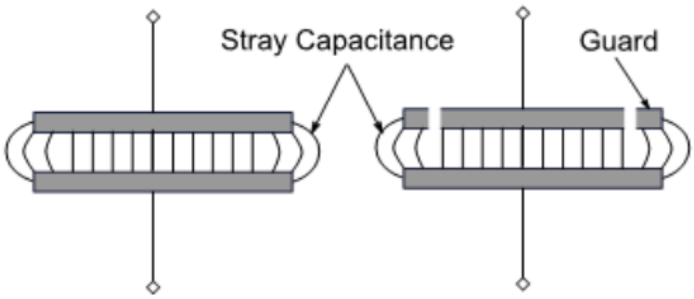

Figure 6.4: Stray capacitance was introduced due to the fringing effect. Guard design to eliminate the fringing effect. *Image by A. Franck, Dielectric Characterization. 2012* [31].

- **Air gaps**: Macro air gaps exist between the two conducting plates and the phantom sample. These are unpreventable and the humidity of air adds to the measured capacitance. Thus, causing a deviation error when compared to the MUT's true capacitance. The error caused by air gaps can be reduced by evaporating a metal film on the surface of the sample. This however does not fully remove them.
- **Piezoelectric effects**: The applied pressure of the conducting plates onto the skin can also cause changes in the conductivity [6]. Applying light to moderate pressure results in a good contact area and more accurate measurements. Applying too much force will cause structure expansion of the gel; causing some misalignment between the contact area of the conducting plates and the MUT. To ensure good contact between the conducting plates and the MUT, the MUT has to be some form of solid rather than a liquid.

There are other parasitic effects present for non-ideal capacitors, but these can be neglected. An example is the equivalent series inductance (ESL) introduced by leads that are connected to the conducting plates of the capacitor. These leads form a pathway to equipment such as an impedance analyser; used to apply a voltage to the capacitor and then measure its impedance. Generally, for low frequencies, this component can be ignored (impedance inductor = $i\omega L$ and converges to 0 for low frequencies).

6.4. Method of approach

A basic homemade capacitor is built with aluminium foil placed on the top and bottom surfaces of the MUT. To try and reduce air gaps, the creases of the aluminium foil are straightened as much as possible with a credit card. A surface area A much larger than the MUT's thickness d is hereby preferred to be able to neglect the fringing effects of the capacitor. The rule of thumb is that fringing is ignored when the ratio length/area is less than 50. The MUTs considered are phantom samples fabricated in the Petri-dishes. Measurements are hereby performed for cylindrical phantoms samples, as the parallel plate method is not applicable for a unique structure such as the human ear. Due to the unavailability of equipment to precisely cut the samples into smaller pieces, the samples are kept at their fabricated size (size of the petri-dish). This equals to a circular contact area A of 113 cm^2 and a MUT thickness d of 8 mm and is in accordance with the rule of thumb to neglect fringing effects (A $\geq$ 50×d). Figure 6.5 shows the sample under test. The two aluminium conductive layers are connected to the impedance analyser using small probe contact extensions. The whole setup is placed in a Faraday cage to mitigate external noise.

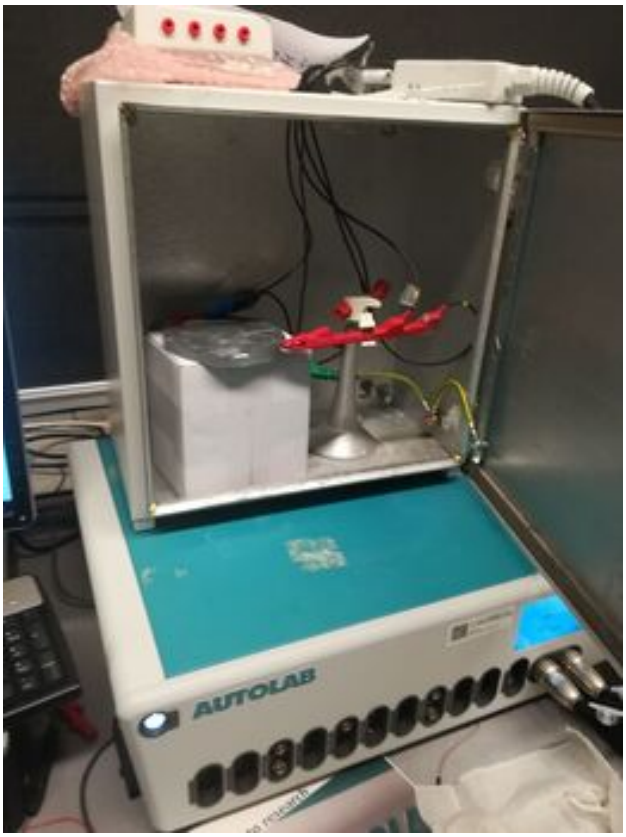

Figure 6.5: Cylindrical phantom sample formed into a parallel plate capacitor with leads, placed in a Faraday cage and connected to an impedance analyser.

An Autolab PGSTAT302N impedance analyser is used to measure the impedance, as it is specially designed for electrochemical impedance spectroscopy. It has a compliance voltage of 30 V and a bandwidth of 1 MHz.
As mentioned in section 3.3, the conductivity of wet skin ranges from 0.1 to 0.2 Siemens in the frequency range of 1 Hz to 1 kHz whereas the permittivity ranges from $5.7 \cdot 10^5$ to $5.2 \cdot 10^5$. The resistance and capacitance are calculated by substituting these values, the contact area A of 113 cm^2 and MUT thickness d of 8 mm into the previously mentioned conductivity and capacitor equations (Equation 6.4 and Equation 6.1). This typically provides a calculated impedance of < 100 kΩ and therefore the serial equivalent circuit (Figure 6.3) can be considered.

The measured impedance obtained from the impedance analyser consists of a real and imaginary parts. These are denoted in Equation 6.5 as R and X respectively.

$$Z = R - iX \tag{6.5}$$

Considering the serial equivalent circuit, this can also be expressed as:

$$Z(f) = R - iX = R + \frac{1}{i2\pi fC} \tag{6.6}$$

The capacitance is then calculated via Equation 6.7

$$C = \frac{1}{2\pi fX} \tag{6.7}$$

Using the measured R and the calculated capacitance C, the conductivity and relative permittivity can be calculated using Equation 6.4 and Equation 6.3 respectively.

7

Discussion of Results

With the MUTs modelled and the measurement technique established, measurements are performed using the Autolab PGSTAT302N impedance analyser. MATLAB is hereby used to perform the permittivity and conductivity calculations on every data point (see section A.1).
The legends of the obtained figures denote the solution # with reference back to Table 5.1

The first results obtained are those of agar only solutions. Specifically, samples with agar and DI (no filler materials) ranging from 1 wt.% agar to 3 wt.% agar with steps of 0.4 wt.%. The results are given in Figure 7.1.

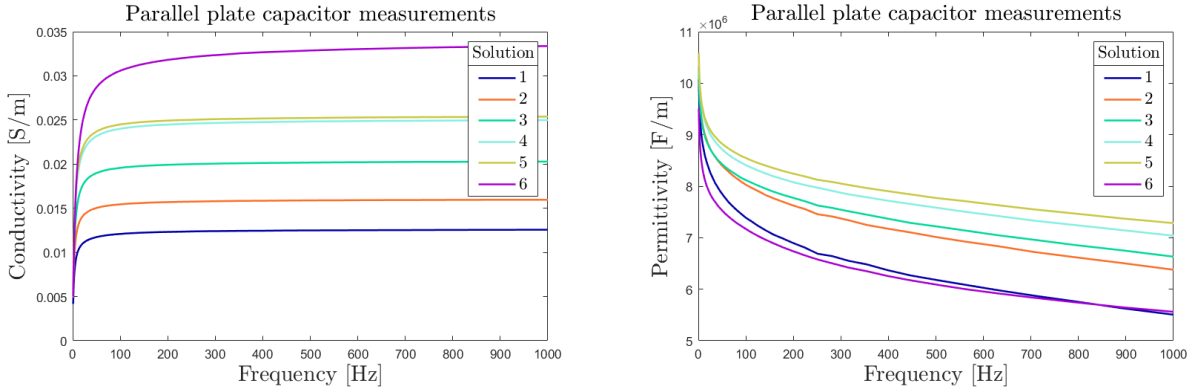

Figure 7.1: Results of the parallel plate capacitor measurements for solutions 1 to 6 of Table 5.1.

It is easy to observe that the conductivity and permittivity increase when more agar is added. This is sensible as deionized water is non-conductive. By adding more agar to the solutions, more material is being added that has conductive and capacitive properties. The sample with 3 wt.% agar (solution #6) is a clear outlier as solutions with 0.4 wt.% agar difference show a similar increase of conductivity. Measurements were retaken for this sample, but the same result was obtained. This is most likely caused by a mistake in the sample fabrication process or when performing the measurements. Possible causes hereby are: a lot of air bubbles are present in the sample, the sample is accidentally fabricated with lower concentrations of agar or the conductive aluminium foil failed to have good contact with the sample.

The next obtained results are those of samples with a constant 3 wt.% agar, DI and NaCl as a filler material in different concentrations. The NaCl concentrations hereby range from 0.5 wt.% up until 1.75 wt.% with steps of 0.25 wt.%. These tests were performed to observe the effect of NaCl concentration on the electric properties of the samples. The results are given in Figure 7.2.

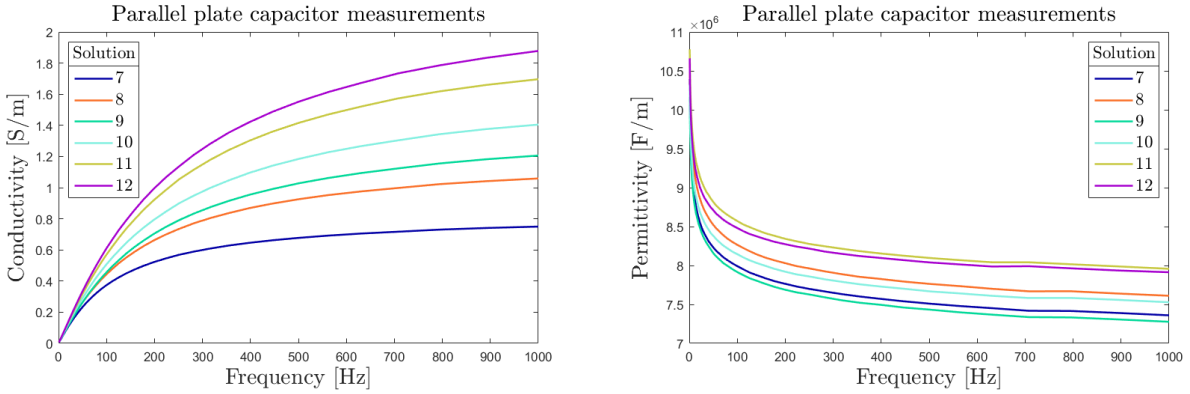

Figure 7.2: Results of the parallel plate capacitor measurements for solutions 7 to 12 of Table 5.1.

NaCl clearly increases both the conductivity and the permittivity. Moreover, the increase is significantly compared to adding agar to DI. The permittivities of solutions #9 and #10 are lower than expected and are most likely outliers. This is most likely also caused by fabrication inaccuracies or noisy measurements. Solution #7 has a conductivity closest to wet skin (0.1 Siemens - 0.45 Siemens versus 0.1 Siemens - 0.2 Siemens) and solution #9 has a permittivity closest to wet skin ($10 \cdot 10^6$ - $7.5 \cdot 10^6$ versus $5.7 \cdot 10^5$ - $5.2 \cdot 10^5$). Both still show quite the marginal difference. By looking at Figure 7.2, there can be estimated that the desired conductivity is obtained when solution #7 has a concentration decrease of 0.250 wt.% NaCl. Thus, obtaining a new solution of 3.04 wt.% agar and 0.289 wt.% NaCl.

An important part of the to be fabricated phantom is that it is reproducible/reuse-able. The next tests performed are therefore the sample behaviour over a span of three days. Samples with a constant 3 wt.% agar, DI and NaCl as a filler material in different concentrations exactly like Figure 7.2 are hereby used. The results are given in Figure 7.3. Here, day 1 is the solid line, day 2 is the dashed line and day 3 is the dotted line.

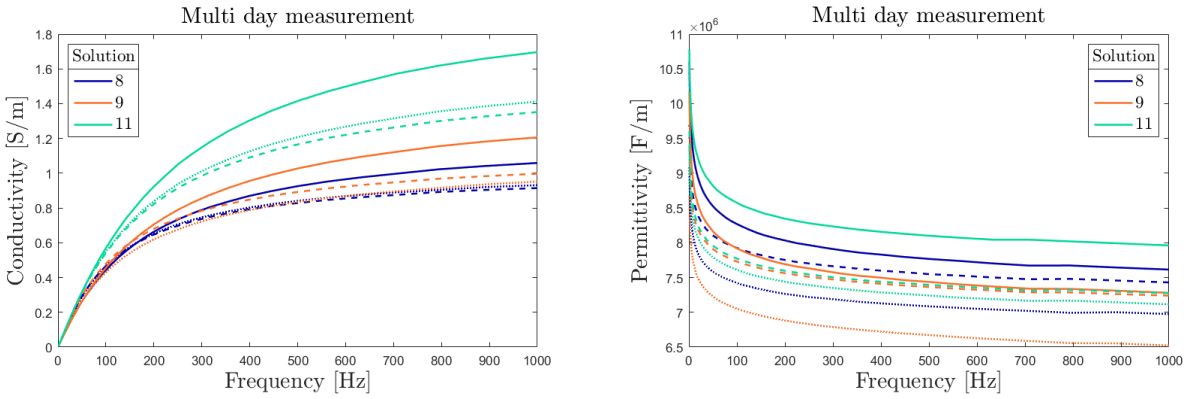

Figure 7.3: Results of multi-day behaviour of a selection of solutions between 7 and 12 of Table 5.1 from day 1 to day 3. Day 1 is the solid line, day 2 is the dashed line and day 3 is the dotted line.

There can be observed that the longer the life-span of the sample, the more the conductivity and permittivity decrease. The most drastic change hereby seems to be between day 1 and day 2 with solution #11 being an outlier. The decrease in electrical properties can be explained by the storing method of the samples. A sample needs to be stored in the fridge at 2°C to mitigate water evaporation. However, it is not possible to mitigate the evaporation completely (therefore losing conductivity). Day

2 and day 3 show very similar properties, so most water evaporation seems to happen between day 1 and 2 and then seems to settle. It also worth mentioning that the shape of the decreased curves are similar for each solution. They just vary on magnitude depending on the value of the conductivity. Specifically, the higher the conductivity, the higher the magnitude of decrease. Small other errors could be present due to noisy measurements or perhaps incorrectly storing the samples.

The last tests performed are those of applied pressure. Samples with a constant 3 wt.% agar, DI and NaCl as a filler material in different concentrations exactly like Figure 7.2 are tested when different pressures are applied to the solutions. The results are given in Figure 7.4. Here, the full line is the original sample with no pressure applied, the dashed line is the sample with pressure applied by a 60g mass and the dotted line is the sample with pressure applied by a 120g mass.

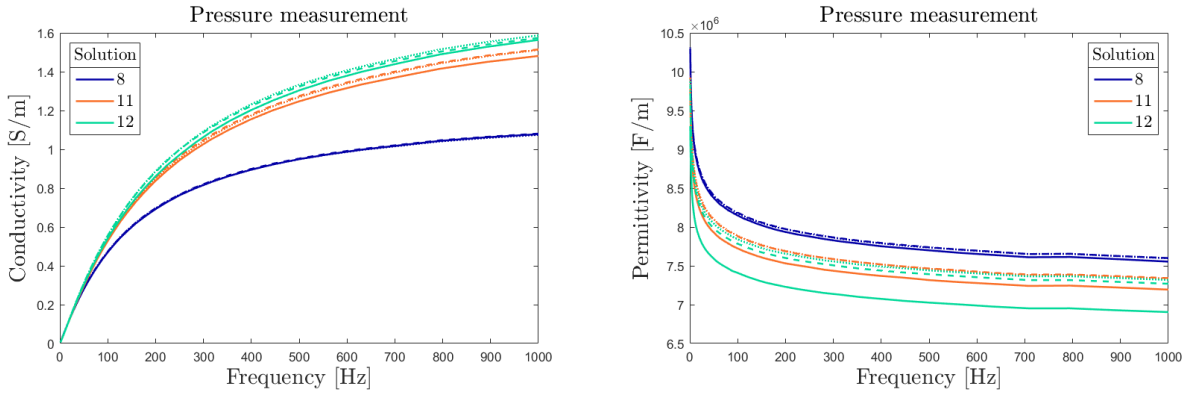

Figure 7.4: Results of pressure test of a set of a selection of solutions between 7 and 12 of Table 5.1 from 0 to 120g.

For the conductivity, a slight increase occurs when pressure is applied. This happens because the weight creates better contact between the aluminium foil and the sample. The permittivity also increases when pressure is applied. This is probably because certain noise gets removed when the weight removes some of the air bubbles. The permittivity of solution #12 is lower than expected and is most likely an outlier caused by erroneous measurements.

8

Conclusion and Recommendations

The goal was to create a skin phantom mimicking the electrical properties of wet human skin. The phantom hereby needed:

- The phantom had to provide a testing ground for dry electrodes used in an ear-EEG BCI (modelling the phantom to be an average sized human ear).
- A conductivity ranging from 0.1 Siemens to 0.2 Siemens in the frequency range of 1-1000 Hz.
- A permittivity ranging from $5.7 \cdot 10^5$ to $5.2 \cdot 10^5$ in the frequency range of 1-1000 Hz.
- To support the idea of reproducibility, the phantom sample had to keep its electrical properties for a span of 7 days.
- A setup is to be used where the influence of applied pressure can be investigated

Although measurements were performed on cylindrical phantoms, an ear-shaped mould is realised using a Creality Ender 3 printer to provide a testing ground for in ear-EEG BCIs. Phantoms hereby consisted of different concentrations of agar and agar/NaCl solutions. Solution #7, containing 3.04 wt.% agar and 0.539 wt.% NaCl, showed most promising in mimicking the conductivity of wet skin. Its obtained values were 0.1 Siemens to 0.45 Siemens in the frequency range of 1-1000 Hz. However, the error of margin is larger than 10% when compared to the desired conductivity range of 0.1 Siemens - 0.2 Siemens. Estimated from the pattern of the results however, a solution much more similar to that of wet skin is obtained when the NaCl concentration is decreased by around 0.250 wt.%. Thus, obtaining a solution with 3.04 wt.% agar and 0.289 wt.% NaCl.
The permittivity was closest realised by solution #9 containing 3.00 wt.% and 1.02 wt.% NaCl. It showed a permittivity of $10 \cdot 10^6$ - $7.5 \cdot 10^6$ in the range of 1-1000 Hz. This also has an error margin larger than 10% when compared to the desired permittivity range of $5.7 \cdot 10^5$ - $5.2 \cdot 10^5$. Adding different fillers could mitigate this error margin, but this was not applicable for this BSc Thesis as there was no availability of a lab to do so.
Multi-day measurements were only performed over a span of 3 days. This is because satisfactory results were obtained. Most drastic changes occurred between day 1 and day 2. There was little change between day 2 and day 3 indicating that most water evaporation occurs on day 1. Moreover, drastic magnitude changes only occurred for solutions with high conductivities. For a solution containing the conductivity of wet skin (0.1 Siemens - 0.2 Siemens), these changes will not be as drastic; thus indicating that the phantom sample keeps its electrical properties for a span of 7 days.
Finally, different known masses were placed on top of the phantoms to investigate the influence of applied pressure. These showed to have little to no effect.

Overall, the results were satisfactory for the most part and two separate phantom solutions, one for conductivity and one for permittivity, can provide a potential testing ground for an ear-EEG BCI. The only problematical issue hereby is having to correct for the phantom related to the permittivity, because it has a large error margin; requiring additional fillers to be added. Improvements and tweaks can be made and these will be discussed below.

8.1. Recommendations

8.1.1. Phantom fabrication

The most important improvement to be made is the decrease of permittivity. Experiments in which other filler materials are added to the phantoms, such as Al powder and glycine, could show if they are suitable for tuning the permittivity of the phantom, as discussed in section 5.1.
Furthermore, the fabrication of the phantom could be handled in a more professional manner to obtain more reliable results. This includes accurate cleaning of the instrumentation, removing air bubbles e.g. using a vacuum, using high-end precision measuring equipment, ensuring a stable room climate, as well as paying attention to water evaporation during the heating process.

8.1.2. Mechanical properties

Next to electrical properties, phantoms can be characterised by their mechanical properties. The two mechanical properties of importance in the electrode-skin interface are the force applied when pressing the electrode against the skin as briefly mentioned in section 3.3, and the elasticity of the material. The elasticity of the material is often modelled via the Young Modulus: the relationship between stress and strain in a material. For human skin, Young's modulus ranges anywhere from 0.42 MPa to 0.85 MPa [18]. Unfortunately, no equipment was available to measure Young's modulus, but doing so can be recommended for future studies with the aim of imitating real human skin even better. The Young Modulus of phantoms can be determined by mounting a phantom sheet sample onto a testing machine and stretching it out with a set amount of force until it breaks.

8.1.3. Improvement of measurement techniques

As mentioned in section 6.3, various parasitic effects occur when trying to measure the electrical properties of phantoms using the contact parallel plate method. One of these was the presence of air gaps between the conducting plates and the sample under test. [30] introduced a non-contact setup for the parallel plate method reducing the influence of the surface conductivity and pressure applied to the conducting plates.
Another possibility could be the use of more advanced equipment. Currently, a simple homemade parallel plate capacitor was used. Equipment such as the Keysight fixture 16451B [28] contains the parallel plate capacitor setup and additionally contains a guard electrode. This is a third electrode placed next to either the top or bottom electrode along with an insulating gap. This is supposed to draw the charge generated from the electric field at the edges and removes the so-called fringing effect/capacitance. In other words, the capacitance measured between the two electrodes is a closer representation of the sample's dielectric properties. Furthermore, it provides an accurate slide bar used to change the distance between the electrodes and the sample and might remove unwanted piezoelectric effects. This fixture is still used in combination with an LCR meter or impedance analyser.

Bibliography

[1] N. Plunkett and F. J. O'Brien, "Bioreactors in tissue engineering", *Technol Health Care*, vol. 19 no. 1, 2011. http://doi.org/10.3233/THC-2011-0605.

[2] M. A. Kandadai, J. L. Raymond and G. J. Shaw, "Comparison of electrical conductivities of various brain phantom gels: Developing a 'Brain Gel Model", *Materials science & engineering. C*, vol. 32 no. 8, 2012. http://doi.org/10.1016/j.msec.2012.07.024.

[3] C. Liu et al., "Microelectromechencial system-based biocompatible artificial skin phantoms", *Micro & Nano letters*, vol. 14 no. 3, pp. 333-338, 2019. http://doi.org/10.1049/mnl.2018.5112.

[4] I. Martin, D. Wendt, and M. Heberer, "The role of bioreactors in tissue engineering", *Trends Biotechnol.*, vol. 22, no. 2, 2004. http://doi.org/10.1016/j.tibtech.2003.12.001.

[5] J. H. Lee et al., "CNT/PDMS-based canal-typed ear electrodes for inconspicuous EEG recording", *J. Neural Eng.*, vol. 11, 2014. http://doi.org/10.1088/1741-2560/11/4/046014.

[6] B. Taji, A. D. C. Chan and S. Shirmohammadi, "Effect of Pressure on Skin-Electrode Impedance in Wearable Biomedical Measurement Devices", *IEEE Transactions on Instrumentation and Measurement*, vol. 67 no. 8, 2018. http://doi.org/10.1109/TIM.2018.2806950.

[7] A. M. R. Pinto, P. Bertemes-Filho1 and A. Paterno, "Gelatin: a skin phantom for bioimpedance spectroscopy", *Biomedical Physics & Engineering Express*, 2015. http://doi.org/10.1088/2057-1976/1/3/035001.

[8] C. Gabriel, S. Gabriel and E. Corthout, "The dielectric properties of biological tissues: I. Literature survey" *Phys. Med. Biol.*, vol. 41 no. 11, pp. 2271-2293, 1996. http://doi.org/10.1088/0031-9155/41/11/001.

[9] S. Gabriel, R. W. Lau and C. Gabriel, "The dielectric properties of biological tissues: II. Measurement in the frequency range 10 Hz to 20 GHz", *Phys. Med. Biol.*, vol. 41 no. 11, pp. 2251-2269, 1996. http://doi.org/10.1088/0031-9155/41/11/002.

[10] S. Gabriel, R. W. Lau and C. Gabriel, "The dielectric properties of biological tissues: III. Parametric models for the dielectric spectrum of tissues", *Phys. Med. Biol.*, vol. 41 no. 11, pp. 2271-2293, 1996.

[11] Y. Fu et al., "Dry Electrodes for Human Bioelectrical Signal Monitoring", *Sensors*, vol 30. no. 13, 2020. http://doi.org/10.3390/s20133651.

[12] S. Hesabgar, R. Jafari and A. Samani,"Accurate Technique for Measuring Electrical Permittivity of Biological Tissues at Low Frequencies and Sensitivity Analysis", *Conference: IEEE International Symposium on Medical Measurements and Applications (MeMeA)*, 2018. http://doi.org/10.1109/MeMeA.2018.8438680.

[13] A. Y. Owda and A. Casson, "Electrical properties, accuracy, and multi-day performance of gelatin phantoms for electrophysiology", *bioRxiv*, 2020. http://doi.org/10.1101/2020.05.30.125070.

[14] W. D. Hairston, G. A. Slipher and A. B. Yu, "Ballistic gelatin as a putative substrate for EEG phantom devices", *Physics. Med.*, 2016. https://doi.org/10.48550/arXiv.1609.07691.

[15] Y. Yu et al., "Tissue phantom to mimic the dielectric properties of human muscle within 20 Hz and 100 kHz for biopotential sensing applications" *Annual International Conference of the IEEE Engineering in Medicine and Biology Society (EMBC)*, vol. 41, 2019. http://doi.org/10.1109/EMBC.2019.8856530.

[16] D. Kim et al., "Validation of Computational Studies for Electrical Brain Stimulation With Phantom Head Experiments", *Brain Stimulation*, vol. 8, pp. 914-925, 2015. http://doi.org/10.1016/j.brs.2015.06.009.

[17] D. Bennett, "NaCl doping and the conductivity of agar phantoms", *Materials Science and Engineering*, vol. 31 no.2, pp. 494-498, 2011. http://doi.org/10.1016/j.msec.2010.08.018.

[18] M. Pawlaczyk, M. Lelonkiewicz and M. Wieczorowski, "Age-dependent biomechanical properties of the skin", *Postepy dermatologii i alergologii*, vol. 30 no. 5, pp. 302-306, 2013. http://doi.org/10.5114/pdia.2013.3835.

[19] T. I. Oh et al., "Flexible electrode belt for EIT using nanofiber web dry electrodes", *Physiol. Meas.*, vol. 33, 2012. http://doi.org/10.1088/0967-3334/33/10/1603.

[20] P. Tallgren et al., "Evaluation of commercially available electrodes and gels for recording of slow EEG potentials", *Clinical Neurophysiology*, vol. 116, pp. 302-306, 2005. http://doi.org/10.1016/j.clinph.2004.10.001.

[21] L. M. Ferrari et al., "Conducting polymer tattoo electrodes in clinical electro- and magneto-encephalography", *Flexible Electronics*, vol. 4 no. 4, 2020. http://doi.org/10.1038/s41528-020-0067-z.

[22] T. J. Yorkey, J. G. Webster and W. J. Tompkins, "Comparing reconstruction algorithms for electrical impedance tomography", *IEEE Trans Biomed Eng.*, vol. 34 no. 11, 1987, http://doi.org/10.1109/tbme.1987.326032..

[23] C. S. Nayak and A. C. Anilkumar, "EEG Normal Waveforms", *Statpearls*, 2022. [Online]. Available: https://www.ncbi.nlm.nih.gov/books/NBK539805/.

[24] Y. M. Chi, T. Jung and G. Cauwenberghs, "Dry-Contact and Noncontact Biopotential Electrodes:Methodological Review", *IEEE Reviews in Biomedical Engineering*, vol. 3, 2010. http://doi.org/10.1109/RBME.2010.2084078.

[25] D. Miklavcic, N. Pavselj, and F. Hart, "Electric Properties of Tissues", *Wiley Encyclopedia of Biomedical Engineering*, 2006. http://doi.org/10.1002/9780471740360.ebs0403.

[26] Y. Yamamoto, T. Yamamoto, and T. Ozawa, "Characteristics of skin admittance for dry electrodes and the measurement of skin moisturisation", *Med. Biol. Eng. Comput.*, vol. 24 no. 1, 1986. http://doi.org/10.1007/BF02441608.

[27] D. Bora and R. Dasgupta, "Various skin impedance models based on physiological stratification", *ET Syst Biol.*, vol. 14 no. 3, 2020. http://doi.org/10.1049/iet-syb.2019.0013.

[28] Keysight, "Measuring Dielectric Properties Using Keysight's Materials Measurements Solutions", *Keysight, Santa Rosa, California, U.S*, 2014. Accessed: May 8, 2022. [Online]. Available: https://www.keysight.com/us/en/assets/7018-03896/brochures/5991-2171.pdf.

[29] O.V. Tereshchenko, F.J.K. Buesink and F. Leferink, "An overview of the techniques for measuring the dielectric properties of materials", *Conference: General Assembly and Scientific Symposium*, 2011 http://doi.org/10.1109/URSIGASS.2011.6050287.

[30] H. Jing, X. Xiangdong and T. Nathaniel, "Non-contact method to reduce contact problems between sample and electrode in dielectric measurements", *High Voltage*, vol. 5 no. 5, 2020. http://doi.org/10.1049/hve.2019.0334.

[31] A. Franck, "Dielectric Characterization", *TA Instruments, New Castle DE, U.S*, 2012. Accessed: May 8, 2022. [Online]. Available: https://www.tainstruments.com/pdf/literature/APN032%20Dielectric%20characterization_V1_ajf_30SEP12.pdf.

[32] J. P. Reilly, "Electrical Stimulation And Electropathology", *Cambridge University Press*, 1992.

[33] K. Wilke et al., "A short history of sweat gland biology", *International Journal of Cosmetic Science*, 2007. http://doi.org/10.1111/j.1467-2494.2007.00387.x.

[34] P. Akshay et al., "Electrode-Skin Impedance Characterization of In-Ear Electrophysiology Accounting for Cerumen and Electrodermal Response". *Conference: International IEEE/EMBS Conference on Neural Engineering (NER)*, 9th, 2019. http://doi.org/10.1109/NER.2019.8716918.

Appendices

A

MATLAB Code

A.1. Calculation of the conductivity and permittivity

```
% Constants
R = 0.06;                          % Radius sample
A = pi*R.^2;                       % Area sample
T = 0.008;                         % Thickness
e0 =  8.854187817*10.^(-12); % Vacuum permittivity

% Frequency Array
F = dataa3000mgn1000mg(:,2);
% TU-Delft colors
colorshex = ["#0300a6","#fa7029","#00d999","#84f0e1","#c8c942","#a700cf
    ","#fa7029","#ebed5c","#75ffad","#0300a6","#00d999"];

% ---Resistance matrices
Reals = [dataa3000mgn750mgd2w12g(:,3) dataa3000mgn1500mgd2w12g(:,3)
    dataa3000mgn1750mgd3w0(:,3)];
Realsd2 = [dataa3000mgn750mgd2w60g(:,3) dataa3000mgn1500mgd2w60g(:,3)
    dataa3000mgn1750mgd3w60g(:,3)];
Realsd3 = [dataa3000mgn750mgd2w120g(:,3) dataa3000mgn1500mgd2w120g(:,3)
    dataa3000mgn1750mgd3w120g(:,3)];

% conductivity
conductivity_d1 = (Reals .^(-1)) * (T/A);
conductivity_d2 = (Realsd2 .^(-1)) * (T/A);
conductivity_d3 = (Realsd3 .^(-1)) * (T/A);

figure
subplot(1,2,1)
hold on
for i = 1:size(conductivity_d1,2)
    % Logarithmic y-axis
    p1 = semilogy(F, conductivity_d1(:,i), '-', 'LineWidth', 1.5);
    p2 = semilogy(F, conductivity_d2(:,i), '--', 'LineWidth', 1.5);
    p3 = semilogy(F, conductivity_d3(:,i), ':', 'LineWidth', 1.5);
    p1.Color = colorshex(i);
    p2.Color = colorshex(i);
    p3.Color = colorshex(i);
end
hold off
```

```
box on

%Style
title("Pressure measurement", 'interpreter', 'latex','fontsize',18);
xlabel("Frequency [Hz]", 'interpreter', 'latex','fontsize',18)
ylabel("Conductivity [S/m]", 'interpreter', 'latex','fontsize',18);
leg = legend('8','','', '11','','', '12','interpreter', 'latex','fontsize
    ',14,'Location','northwest');
title(leg,'Solution', 'interpreter', 'latex','fontsize',14);

% ---Reactance
Imagsd1 = [dataa3000mgn750mgd2w12g(:,4) dataa3000mgn1500mgd2w12g(:,4)
    dataa3000mgn1750mgd3w0(:,4)];
Imagsd2 = [dataa3000mgn750mgd2w60g(:,4) dataa3000mgn1500mgd2w60g(:,4)
    dataa3000mgn1750mgd3w60g(:,4)];
Imagsd3 = [dataa3000mgn750mgd2w120g(:,4) dataa3000mgn1500mgd2w120g(:,4)
    dataa3000mgn1750mgd3w120g(:,4)];

F_part = (F .^-1) * (1/(2*pi));

% Permittivity from capacitance
for j = 1:size(Imagsd1,2)
    C1 = F_part .* (Imagsd1(:,j) .^ -1);
    permittivity1(:,j) = C1 .* (T/(A*e0));

    C2 = F_part .* (Imagsd2(:,j) .^ -1);
    permittivity2(:,j) = C2 .* (T/(A*e0));

    C3 = F_part .* (Imagsd3(:,j) .^ -1);
    permittivity3(:,j) = C3 .* (T/(A*e0));
end

subplot(1,2,2)
hold on
for k = 1:size(permittivity1,2)
   %logarithmic y-axis
    f1 = semilogy(F, permittivity1(:,k), '-', 'LineWidth', 1.5);
    f2 = semilogy(F, permittivity2(:,k), '--', 'LineWidth', 1.5);
    f3 = semilogy(F, permittivity3(:,k), ':', 'LineWidth', 1.5);
    f1.Color = colorshex(k);
    f2.Color = colorshex(k);
    f3.Color = colorshex(k);
end
hold off
box on

%Style
title("Pressure measurement", 'interpreter', 'latex','fontsize',18);
xlabel("Frequency [Hz]", 'interpreter', 'latex','fontsize',18);
ylabel("Permittivity [F/m]", 'interpreter', 'latex','fontsize',18);
leg = legend('8','','', '11','','', '12', 'interpreter', 'latex','
    fontsize',14);
title(leg, 'Solution', 'interpreter', 'latex','fontsize',14);
```